ARMY RESEARCH LABORATORY

Scalable Coupling of Multiscale AEH and PARADYN Analyses for Impact Modeling

by Rama R. Valisetty, Peter W. Chung, and Raju R. Namburu

ARL-TR-3512 **June 2005**

NOTICES

Disclaimers

The findings in this report are not to be construed as an official Department of the Army position unless so designated by other authorized documents.

Citation of manufacturer's or trade names does not constitute an official endorsement or approval of the use thereof.

Destroy this report when it is no longer needed. Do not return it to the originator.

Army Research Laboratory
Aberdeen Proving Ground, MD 21005-5067

ARL-TR-3512 **June 2005**

Scalable Coupling of Multiscale AEH and PARADYN Analyses for Impact Modeling

Rama R. Valisetty, Peter W. Chung, and Raju R. Namburu
Computational and Information Sciences Directorate, ARL

Report Documentation Page

Form Approved
OMB No. 0704-0188

1. REPORT DATE *(DD-MM-YYYY)*	2. REPORT TYPE	3. DATES COVERED (From - To)
June 2005	Final	2003–2004

4. TITLE AND SUBTITLE
Scalable Coupling of Multiscale AEH and PARADYN Analyses for Impact Modeling

5a. CONTRACT NUMBER

5b. GRANT NUMBER

5c. PROGRAM ELEMENT NUMBER

6. AUTHOR(S)
Rama R. Valisetty, Peter W. Chung, and Raju R. Namburu

5d. PROJECT NUMBER
5UH7FL

5e. TASK NUMBER

5f. WORK UNIT NUMBER

7. PERFORMING ORGANIZATION NAME(S) AND ADDRESS(ES)
U.S. Army Research Laboratory
ATTN: AMSRD-ARL-CI-HC
Aberdeen Proving Ground, MD 21005-5067

8. PERFORMING ORGANIZATION REPORT NUMBER
ARL-TR-3512

9. SPONSORING/MONITORING AGENCY NAME(S) AND ADDRESS(ES)

10. SPONSOR/MONITOR'S ACRONYM(S)

11. SPONSOR/MONITOR'S REPORT NUMBER(S)

12. DISTRIBUTION/AVAILABILITY STATEMENT
Approved for public release; distribution is unlimited.

13. SUPPLEMENTARY NOTES

14. ABSTRACT
This report describes scalable coupling of two stand-alone computer codes for a multiscale impact analysis of composites. An asymptotic expansion homogenization (AEH)-based microstructural model available for modeling microstructural aspects of modern armor materials is coupled with PARADYN, a parallel explicit Lagrangian finite-element code. The first code enables modeling of a material microstructure and provides material response in terms of global structural response at a material integration point. Microstructural codes such as this one are typically used in stand-alone form and applied in simple loading situations. The coupling provided here enables a micro/macro type multiscale analysis under generalized three-dimensional loading conditions. Three sets of results are presented to demonstrate: (1) the verification of the AEH-PARADYN model coupling to PARADYN, (2) the scalability of the coupled model, and (3) an application for modeling the impact response of armor materials. In the present work, a consistent AEH numerical formulation was selected that was earlier shown to be scalable on different computing architectures. In conjunction with a second-order accurate velocity-based explicit time integration method, the formulation is coupled within the message-passing interface scheme of PARADYN. PARADYN is a scalable version of the Lawrence Livermore National Laboratory's serial DYNA3D explicit Lagrangian finite-element code used for obtaining large deformation, elastic/plastic response of structures.

15. SUBJECT TERMS
AEH, PARADYN, HPC, scalable computing, impact modeling

16. SECURITY CLASSIFICATION OF:			17. LIMITATION OF ABSTRACT	18. NUMBER OF PAGES	19a. NAME OF RESPONSIBLE PERSON
a. REPORT	b. ABSTRACT	c. THIS PAGE			Rama R. Valisetty
UNCLASSIFIED	UNCLASSIFIED	UNCLASSIFIED	UL	44	19b. TELEPHONE NUMBER (*Include area code*) 410-278-6638

Standard Form 298 (Rev. 8/98)
Prescribed by ANSI Std. Z39.18

Contents

List of Figures

List of Tables

INTENTIONALLY LEFT BLANK.

1. Introduction

Heterogeneous materials, such as layered or dispersed particulate composites, are widely used in military armor applications for protection from ballistic impacts or for defeating enemy structures and vehicles. For effective use of these materials in short duration impact applications, one should be able to quantify the local- or microlevel structural response of the constituent phases, understand the different failure modes at the microstructural level, and translate this information into the effective constitutive material properties at the global level.

Spanning a heterogeneous material from its component microphases to its global structural level with finite elements to obtain micro- and global structural responses leads to large finite-element meshes and computations that are both expensive and intractable. Multiscale analyses are used to alleviate this problem and are even being extended to include nanoscale analyses to aid nanomaterial development.

At a basic level, these analyses use one or more microstructural models for describing microlevel material features, such as fibers, particles, lamina, voids, etc., and express the microlevel response as a local perturbation of global response. Each element, or a selected few of the global elements, calls the microstructural model to sample the microlevel structural response and build the element level stresses.

While many theories are available for linking the microstructural response to the global response, the theory selected here is capable of modeling elastic/plastic large deformation seen in the armor impact applications. It is based on the mathematically rigorous asymptotic expansion homogenization (AEH) method. While a historical context to it is presented in the next section, its most recent proponents are Chung et al. (1999), who extended its range of application to include short transient loading and applied it for predicting the elastic/plastic large deformation of composite materials.

In the AEH approach, the microlevel response is expressed in terms of the global response in a strict, mathematically seamless approach. An updated Lagrangian scheme for small strains and small rotations is employed to account for large displacements, strains, and rotations over many time steps. At each time step, the equilibrium solution from the previous time step is used to update the local microstructure.

Since explicit time integrations take quite a large number of time steps and microlevel computations are to be performed at each and every time step and for the selected global finite elements, the attendant micro computations can take much longer times for solution. Scalable computational approaches are needed to use these computationally intensive methods. With the aid of domain decomposition and message-passing interface (MPI), the basic equations of

Chung et al. (1999) were recast for parallel computation and were shown to be scalable for a Taylor impact of a laminate with several hard and soft layers by Valisetty (2000).

While the previous two references used the microstructural AEH as a stand-alone code, the current work couples it as a material level response provider to PARADYN, a general purpose explicit dynamics code. The objective was to extend the applicability of AEH to large-scale multi-material impact analyses. PARADYN is a parallel version of the Lawrence Livermore National Laboratory's serial DYNA3D code. It is a natural choice for the present purpose because of its large number of material models, contact algorithms, element types, etc.

Coupling two stand-alone structural codes, such as the microstructural AEH and PARADYN, is best accomplished when the interface computer code is written in a form that is as simple as possible. While an independent stand-alone interface is desirable, it has to accomplish two objectives: (1) the data exchange between the two codes must be transparent to users, and (2) the coupling to the driver code, i.e., PARADYN, must be done in such a way that it does not disturb any of the driver code's special features, such as scalable parallel operations, time integration, contact algorithms, etc.

Since PARADYN is a scalable parallel code, it already has its computational logic and data structures set for tackling parallel computations. Even though the code has facilities to add user-defined materials and elements, the present microstructural AEH is neither a new material nor an element. Since potentially large microstructural element models can be considered with the microstructural AEH, requiring large amounts of microelement specific material properties, stresses and strains data to be stored and made available for conducting time integration, using PARADYN's data arrays for storing and retrieving such microelement data becomes intractable and potentially conflicting to its scalability operations. To alleviate this situation, external processor specific files are used for writing a global element's data and microstructural elements' data. This enables the AEH model coupling without disturbing the PARADYN code's MPI and domain decomposition-based scalability operations.

To enable access to the microstructure AEH model, a reference is provided to it as a "Material Type 3" sub-option in PARADYN. This reference is completely arbitrary and could be placed even without getting into any material level subroutines. Global elements tabbed with this material option then write the current time step and strain increment data to external files and read back the effective mechanical properties and effective stresses. With the aid of a user-specified microelement finite-element model and after reading global elements' data, the AEH model conducts microlevel analyses and writes the effective properties and stress data to files. The data exchange between the PARADYN and AEH codes occurs through external processor specific files. Thus, with this interface, a dual level finite-element modeling capability is added to the PARADYN code.

With regards to writing the computer code of the interface, while many environments are available, the one that was considered is the "interdisciplinary computing environment (ICE)."

As described by Clarke and Namburu (2002), this environment uses an "extensible data model and format (XDMF)" for describing the nature of data being exchanged between the codes and a visual environment for the user to monitor the exchanging data while the codes run independently in the background. The xdmf uses extensible markup language (XML), hierarchical data format version 5 (HDF5), and network distributed global memory (NDGM). The XML language uses PYTHON language script to enable users to describe the types of data being exchanged between the independently running codes. The HDF5 data format in which the codes exchange data via external files is an effective format not only for doing read/writes but also for grouping the data for fast scientific visualization. The NDGM provides data access to codes running on processor grids in a scalable manner.

While the ICE experience of data markup, visualization, storage, and handling will be discussed in a future publication, the usefulness of the AEH-PARADYN coupling is presented in the current report. When coupled with PARADYN, the microstructural AEH can potentially avail the various material models for its constituent materials from PARADYN. Also, in application runs, PARADYN's features (e.g., contact and the ability to remove excessively deformed global materials) can also be used. The microstructural AEH enhancement of PARADYN was demonstrated through simulation of plate impact tests for three composite laminates made of extremely dissimilar materials.

The outline of this report is as follows. Section 2 presents a brief historical context to the AEH development. Section 3 presents the details of the microstructural AEH coupling to PARADYN and guidelines for its use. Section 4 presents verification, scalability, and application of the coupled codes. The micro- and global structural response coupling and equations are presented in the appendix.

2. AEH Development

While the rule of mixtures represents an earliest concept in composite micromechanics, the idea that stress/strain distributions caused by holes and inclusions in an otherwise uniform medium can be used to represent the stress/strain distributions around fibers in laminas is the starting point for the development of homogenization theories. Licht Frottement (1987), Lene (1984), Moulinec and Suquet (1994), Bensoussan et al. (1978), and Sanchez-Palencia (1980) have formalized the mathematics of the homogenization theories for obtaining the effective material properties. The works of Hashin (1962), Hashin and Strickman (1963), Hill (1964), Willis (1982), and Suquet (1982) can be seen as the engineering counterparts of these theories.

For a short transient impact loading condition, a detailed knowledge of the material flow in and around material microstructural constituents and material interfaces is necessary. This flow is three-dimensional and elastic/plastic. Classical rule of mixtures theories based on constant stress

or strain assumptions lead to an aggregation of the response in the microstructural details and thus are of limited use.

Recent advances in mathematically rigorous AEH methods enable the coupling of micro- and global approaches for both linear and nonlinear structural applications (Fish et al., 1997; Terada and Kikuchi, 1995; Ghosh and Moorthy, 1995; Lene, 1986; and Guedes and Nikuchi, 1990). Most recently, Chung et al. (1999) demonstrated the applicability of the AEH method for heterogeneous media subjected to short transient loading by employing explicit dynamics finite-element formulations in conjunction with elastic/plastic material response. The investigation of Chung et al. (1999) considers the dynamic equation of motion discretized according to a second order accurate scheme presented in Namburu (1991).

Using the AEH approach, the microlevel variables are expressed as direct functions of the global variables in a strict, mathematically seamless approach. This method is especially suitable for conducting explicit transient elastic/plastic analysis of heterogeneous materials. An updated Lagrangian scheme for small strains and small rotations is employed to account for large displacements, strains, and rotations over many time steps.

Because an explicit time integration scheme takes quite a large number of time steps and the global and microlevel computations are to be performed at each time step and for each global finite element, the attendant micro and global computations can take much longer times for solution. Scalable computational approaches are needed to explore these computationally intensive methods. In Chung et al. (1999), the microstructural AEH was made parallel in a stand-alone explicit dynamics code with results showing good scalability for the AEH's coupled micro/macro equations. These equations are presented in the appendix. They form the basis of the microstructural AEH that is now coupled with PARADYN.

3. Coupling the Microstructural AEH Model in PARADYN

PARADYN is a general-purpose explicit dynamics code with a capability for defining multiple element types and material types. Each element of the global finite-element model that is tabbed for detailed microlevel analysis is made to call the microstructural AEH model to sample the local microlevel behavior and build the element global stresses from the constituent microstresses.

3.1 Guidelines for Using the Model

The microstructural AEH sub-option can be invoked by specifying a "Material Type 3" and a non-zero number in the fifth data location on the eighth material card. The material option

describes a nonlinear elastic/plastic response with kinematic and/or isotropic hardening. The added microcode is not limited to microphase materials of this type, however.

The microstructure is next defined with the usual nodes, elements, and material properties. Although any type of format can be used for this purpose, the one that is selected uses the same PARADYN input format. This was done to avail PARADYN's preprocessors, such as INGRID. Although not verified, at present there are no restrictions on the number of microstructural elements, nodes, and materials.

All the information defining the microstructural AEH is to be contained in an input file separate from the PARADYN's global structure-defining input file and is to be made available to the PARADYN executable along with a domain decomposition part file.

3.2 Details of the Data Exchange

While PARADYN focuses on global computations such as the aggregation of nodal forces, solution of the equations of motion, updating global nodal positions, enforcing contact, etc., the microstructural AEH code focuses on the microstructural AEH calculations which typically involve evaluating the microstructure as a perturbation of global deformation and periodicity. For the two codes to perform their respective computations, it is necessary that the relevant data be exchanged between them for each time step and for each global element identified for microcomputations. In the present work, the data exchange involves two parts as follows:

1. From PARADYN, at the beginning of each time step and for the identified global elements, the following data is written to external processor-specific data files for read access to the microstructural AEH model:

   Current time step,

   current global strain increments,

   global strains from previous time step,

   global stresses from previous time step, and

   effective plastic strain from previous time step.

2. After reading the PARADYN-written data files, the microstructural AEH code computes and writes the following data to external processor-specific data files for read access to PARADYN:

   Effective density,

   effective bulk modulus,

   effective shear modulus,

computed current global stresses for the element, and

computed current effective plastic strain for the element.

While PARADYN's native arrays are used for tracking global stresses, global strains, effective properties (density, bulk modulus, and shear strain), and effective plastic strain, no such native arrays are used to store the microelement quantities. Instead, the microelement data are written to, and read from, processor-specific files during each time step and updated. As opposed to the global stresses of the global elements, the stored values of these responses reflect the accurate stress distribution within the microelements of the microstructure. During a PARADYN run, or after the run is complete, the processor-specific files can be visualized independently to analyze the microstructural stress and deformation development for any of the global elements.

4. Results

Verification of the coupling algorithm, evaluation of the coupling scalability, and validation of the coupled codes were achieved through the following numerical analyses conducted on the U.S. Army Research Laboratory's SGI O2k machines.

4.1 Verification of the Model Insertion

For verifying the model coupling, a small cylinder with homogeneous material was considered in a Taylor impact, and was analyzed alternatively as a heterogeneous material with DYNA3D and as a homogeneous material with alternating layers of two different materials but with same identical properties using the microstructural AEH in PARADYN. The idea was that the AEH model should default into a homogeneous material solution, and the data exchange can point to any errors in the coupling.

Enforcing quarter symmetry on sides parallel to the axis of the cylinder, a 90° wedge of the cylinder was considered with 108 elements in five rows, as shown in figure 1. The length and radius of the cylinder was 2.592 mm and 3.2 mm, respectively. The material was considered elastic/plastic with isotropic hardening. The material properties are shown in table 1.

Table 1. Material properties.

Density (kg/m^3)	Young's Modulus (GPa)	Poisson's Ratio	Yield Stress (GPa)	Tangent Modulus (GPa)
8930	117	0.35	0.4	0.1

The velocity of the cylinder was 227 m/s. To affect the deformation, one end of the cylinder was assumed to be free of velocity. Results for axial velocity, axial stress, and effective plastic strain are considered for three nodal locations, near the free end, center, and at the impacted end, as shown in figure 1. They are presented in figures 2–4, respectively, for the heterogeneous

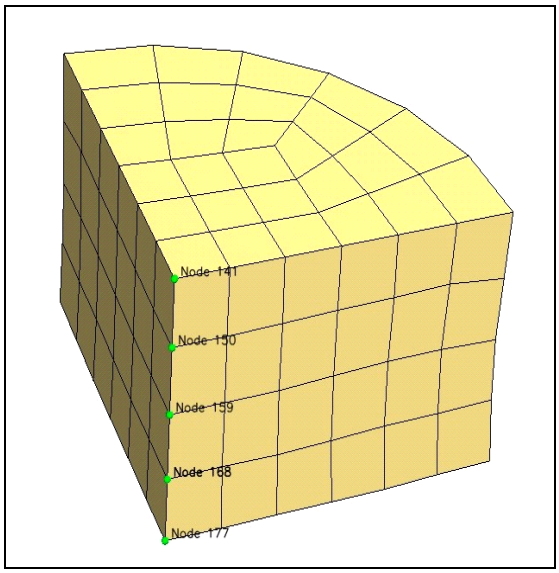

Figure 1. Finite-element mesh of a cylindrical wedge under Taylor impact.

DYNA3D solution and for the homogeneous microstructural AEH-PARADYN solution. Both solutions appear to be in agreement with each other, thus verifying the model coupling for microstructures with homogeneous materials.

4.2 Validation of the Model

In this example, a cylinder similar to the one in the previous example was considered but with two materials alternating in a total of 96 layers normal to the cylinder axis. The length and radius of the cylinder were 31.1 mm and 3.2 mm, respectively. The material was considered elastic/plastic with isotropic hardening. The material properties are shown in table 2.

Table 2. Material properties.

Layer	Density (kg/m^3)	Young's Modulus (GPa)	Poisson's Ratio	Yield Stress (GPa)	Tangent Modulus (GPa)
1	8930	117e9	0.35	0.4e9	0.1e9
2	8930	90e9	0.35	0.4e9	0.1e9

Two solutions were obtained. The first solution was a heterogeneous DYNA3D solution obtained using 10,368 global elements. To model the repeating 48 sets of the two dissimilar materials, eight rows of elements were used for each material layer. The second solution was the homogeneous microstructural AEH-PARADYN solution obtained with a 1296 element global model. The elements are stacked in 96 layers. In contrast to the first solution, a single layer of elements was used for each material. All layers are assumed to be exhibiting homogeneous composite behavior in the global sense, but with microstructural AEH computed using a two-layer microstructural model.

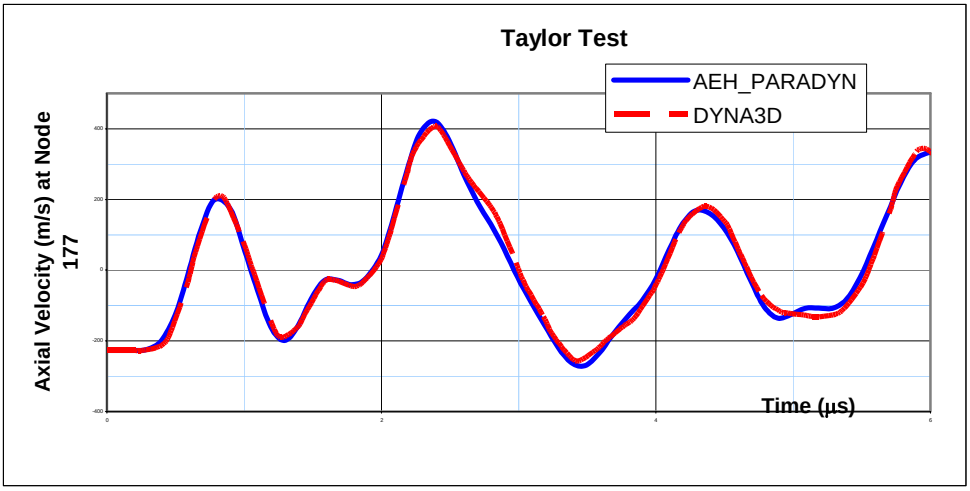

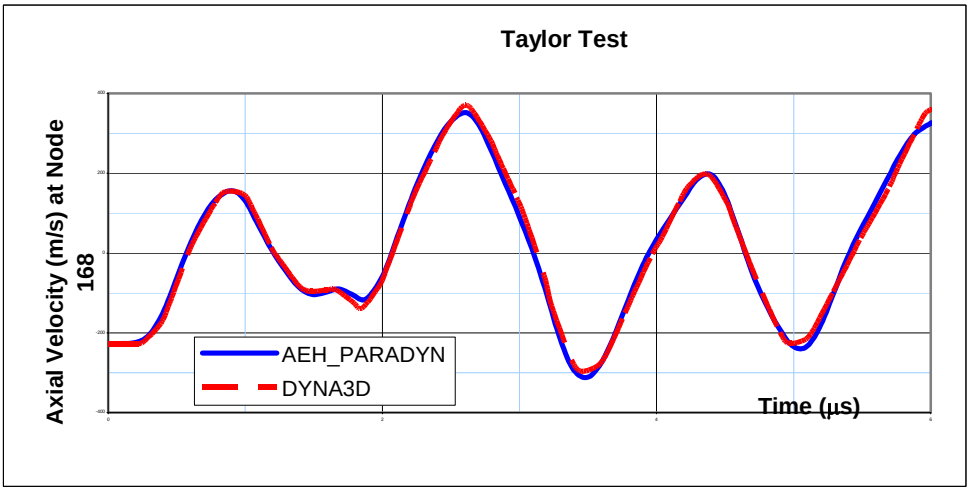

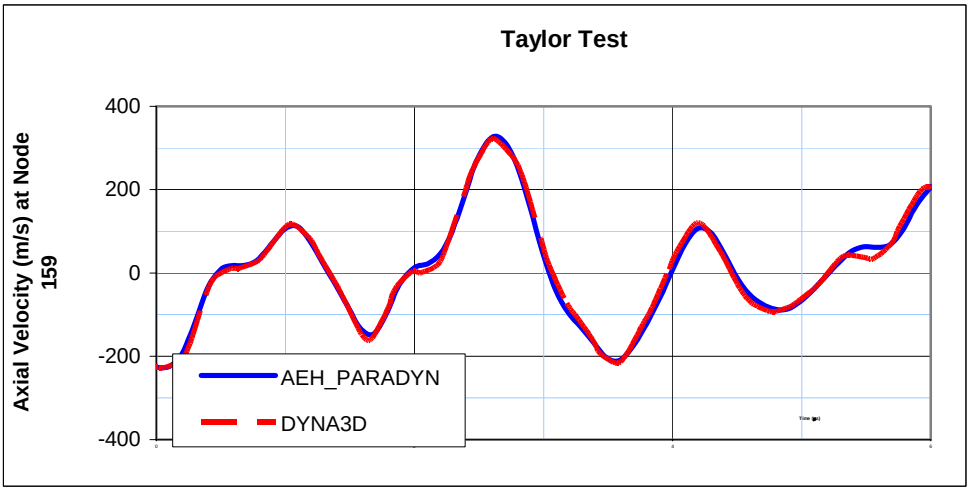

Figure 2. DYNA3D and AEH-PARDYN axial velocity solutions for the finite-element mesh of figure 1.

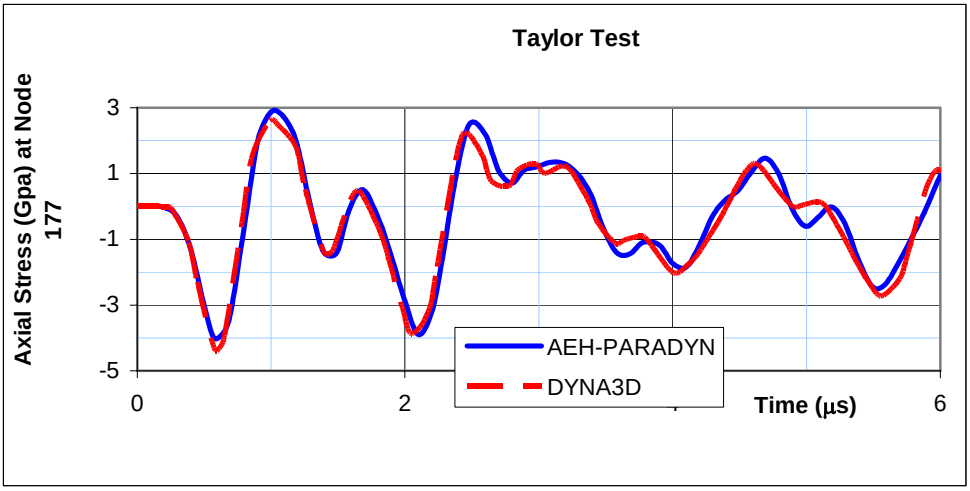

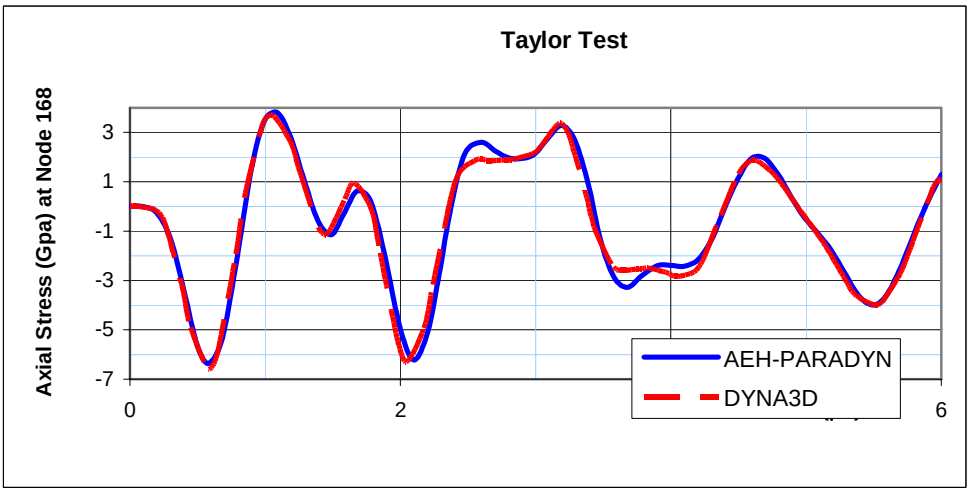

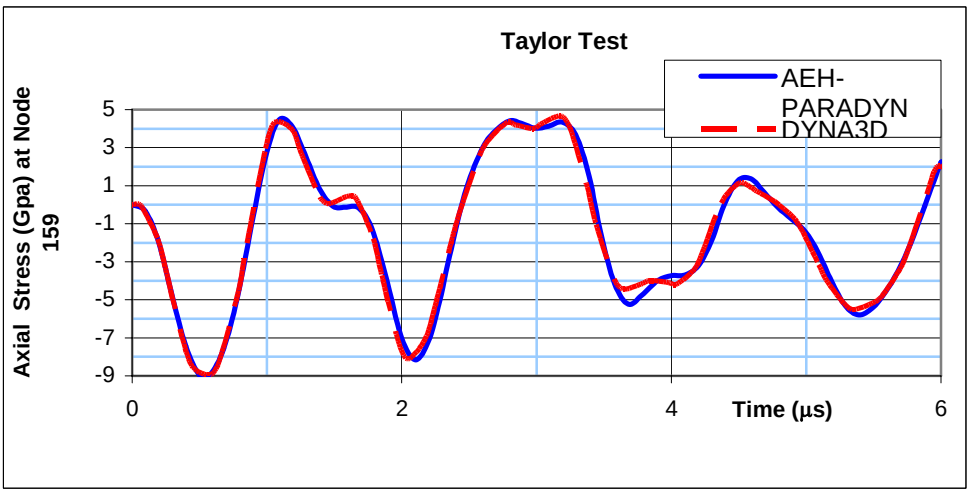

Figure 3. DYNA3D and AEH-PARDYN axial stress solutions for the finite-element mesh of figure 1.

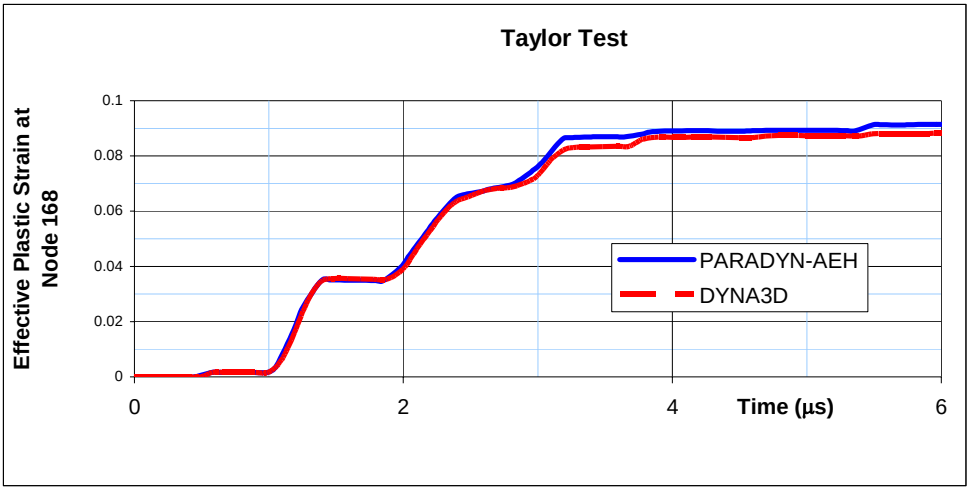

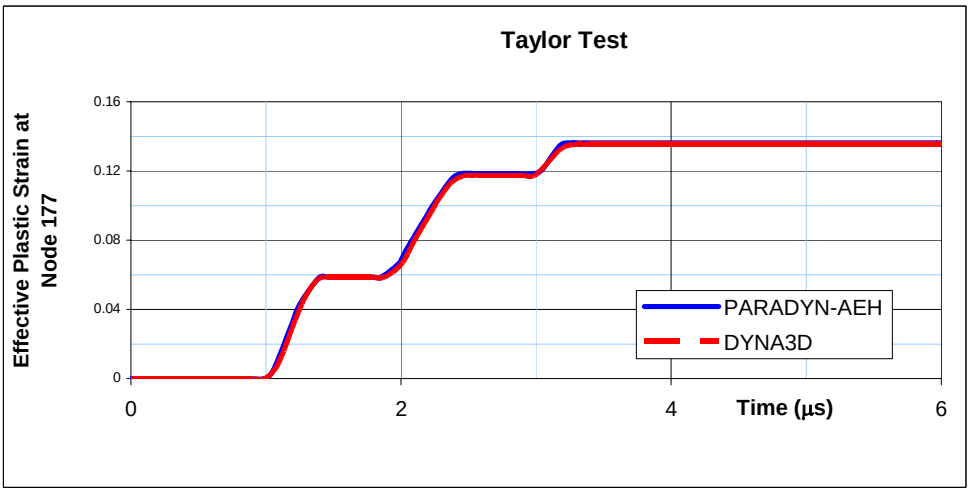

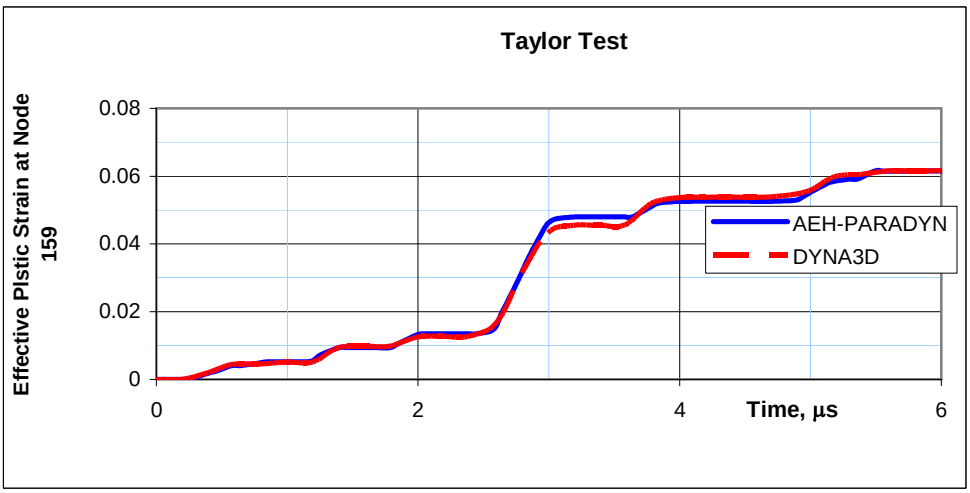

Figure 4. DYNA3D and AEH-PARDYN effective plastic strain solutions for the finite-element mesh of figure 1.

Enforcing quarter symmetry on sides parallel to the axis of the cylinder, a 90° wedge of the cylinder was considered. The velocity imposed on all but one end face of the cylinder is 227 m/s. Figures 5 and 6 show the two models both before and after the impact. Solutions at nodes near top, center, and bottom of the cylinder are presented in figures 7–10, for axial velocity, axial stress, effective stress, and effective plastic strain. For all these responses, the microstructural AEH was able to track the DYNA3D's heterogeneous responses well. Deviations in the axial velocity and axial stress can be attributed to three factors: (1) these differences are near stress-free edges prone to be affected by the transients; (2) the meshes are different in their coarseness which affects the time integration in the two solutions; and (3) the values are node averaged but the nodes are at different locations in the two models since the meshes are different. Similarly, the differences in the plastic strain predictions can be attributed to the extreme length of the time duration of the analysis, which makes the differences accumulate.

4.3 Scalability of the Results

During the development of the AEH-PARADYN coupling interface, due consideration was given to the fact that PARDYN is a parallel code while coupling the microstructural AEH. Because the PARADYN code has a well tested MPI/OPENMP-based computational logic, the coupling was done by keeping a global element's microstructural AEH computations local to the processor on which the global element resides. This means that information such as microelement stresses, strains, and mechanical properties needed in microelement computations are kept local and not passed into global data structures. Consequently, a global element's microstress, microstrain, and micromechanical properties are needed to be written to, and read from, processor-specific files in between time steps. To demonstrate the fact that the penalty associated with this approach is small, results from a limited scalability study are presented in this section.

The Taylor impact model of section 4.2 is used for this purpose. Two types of scalability studies, one with a fixed mesh for standard scalability, and the other with varying mesh size, but with a fixed number of elements per processor, are performed. The nodes, elements, and wall clock times from these studies are presented in table 3. In these simulations, the increase in number of elements was achieved by adding element rows in the cylindrical axis direction only, and not in the hoop and radial directions.

The wall clock times are also plotted in figure 11. The plot on the left side of this figure shows run times for the 122,880 element mesh for the standard scalability study. A linear speedup can be discerned from this plot.

On the other hand, the plot on the right side of the figure shows the run times for the scaled scalability study. In this study, the mesh size was doubled with each doubling of the processors. The run times did not remain constant as were the number of elements per the processor. The

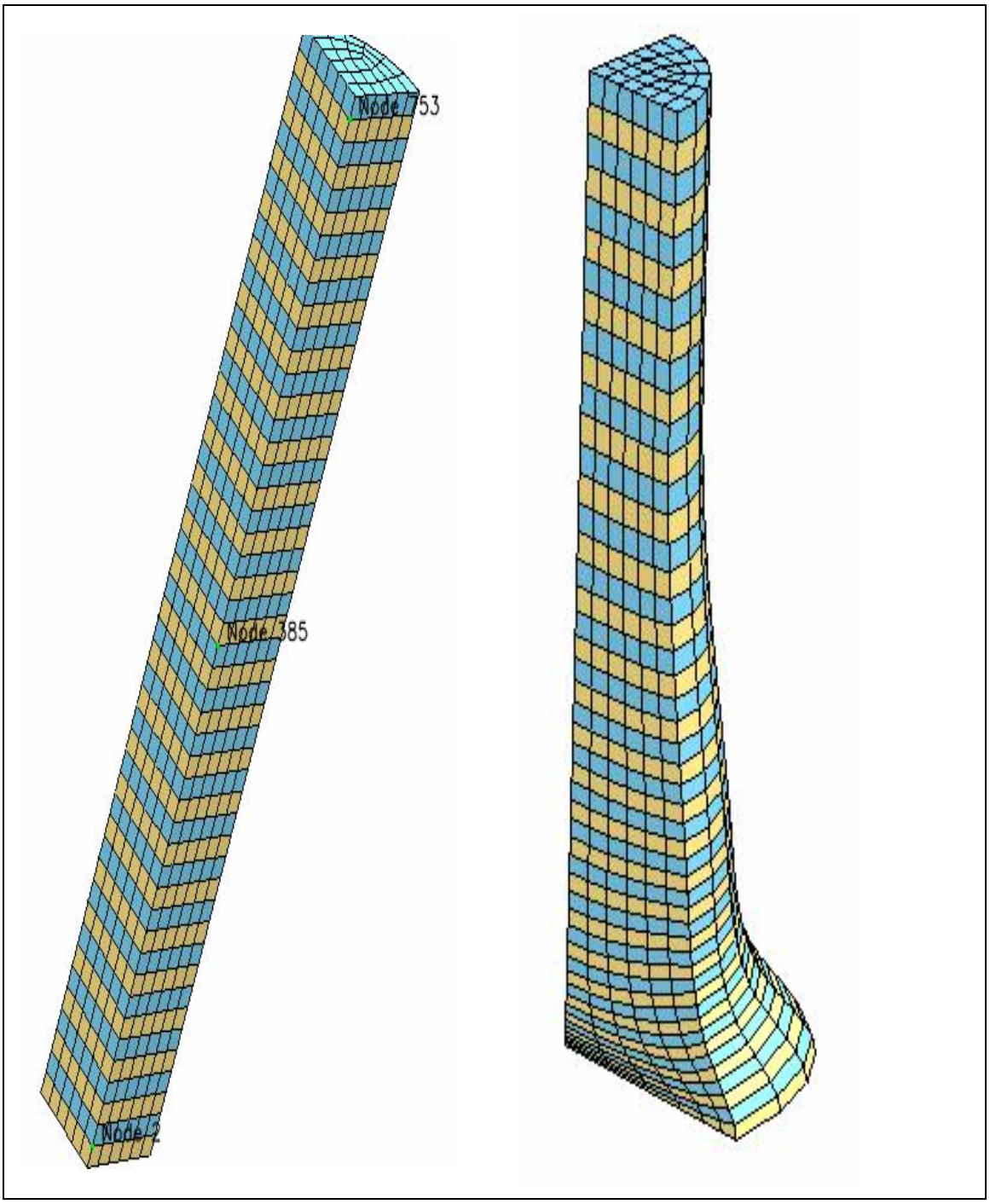

Figure 5. Finite-element model and deformed mesh used for the AEH-PARDYN solution for the verification problem.

reason could be that the plastic deformation is very concentrated near base and the domain decomposition used to distribute the elements over processors is not sensitive to this fact. Another factor could be the small processor load (~2000 elements/processor). The scalability might improve with a higher processor load (e.g., 20,000 elements/processor or higher).

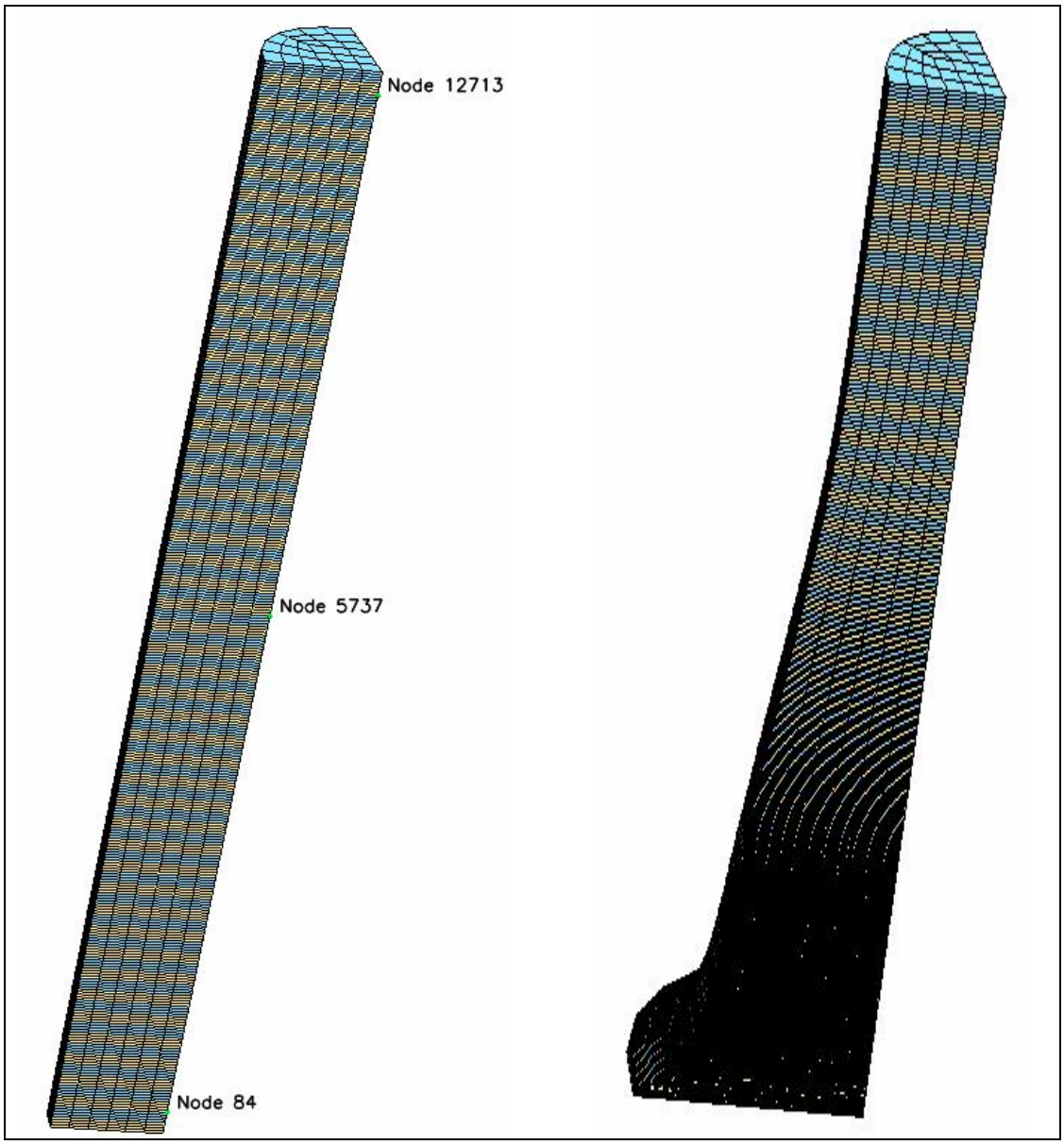

Figure 6. Finite-element model and deformed mesh used for the DYNA3D solution for the verification problem.

4.4 An Application of the Model

In this section, the ability of the microstructural model AEH-PARADYN to predict the experimentally observed impact behavior of laminates with widely dissimilar and alternating layers of materials is demonstrated. For this purpose, impacts of three composite laminates from the experimental work of Zhuang (2002) are considered. In all these impacts, the objective was to study the effect of composite lay-ups with alternating hard and soft layers on shock wave propagation. Capturing the local mechanical behavior of such lay-ups is very difficult, especially in the regime of shock.

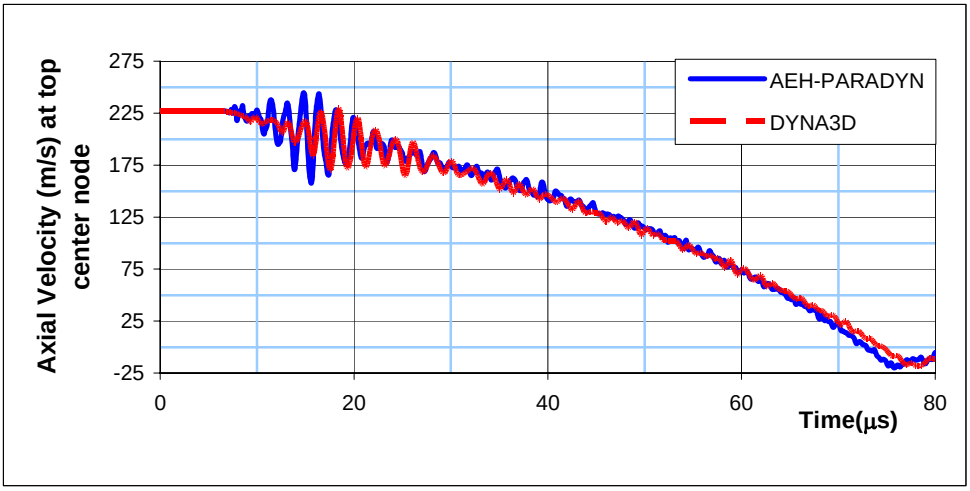

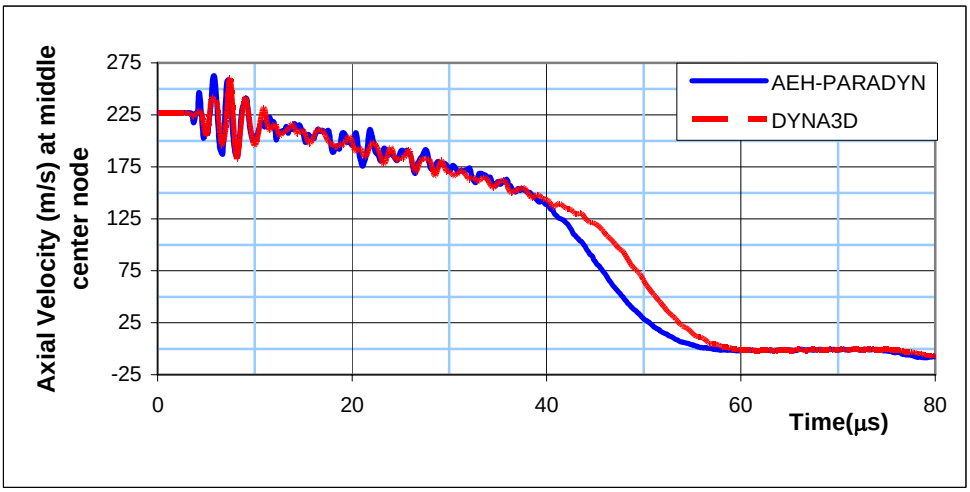

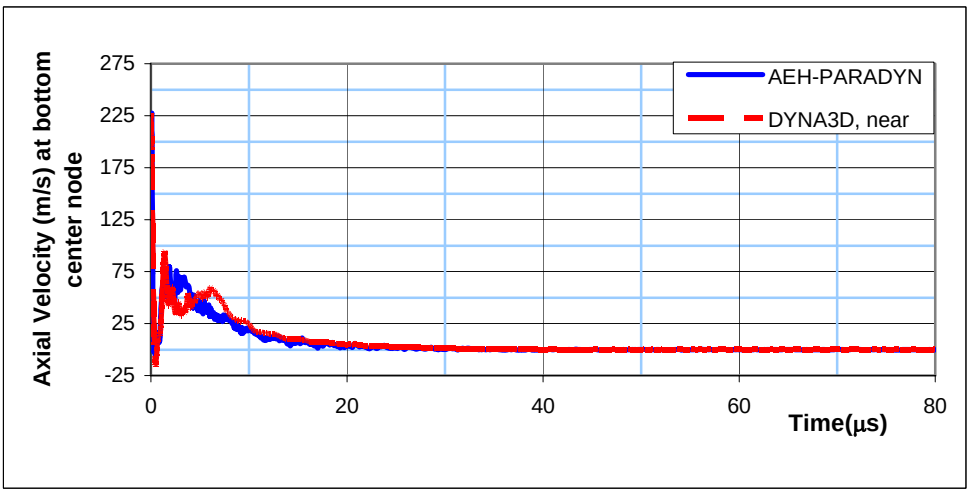

Figure 7. DYNA3D and AEH-PARDYN axial velocity solutions for the validation problem.

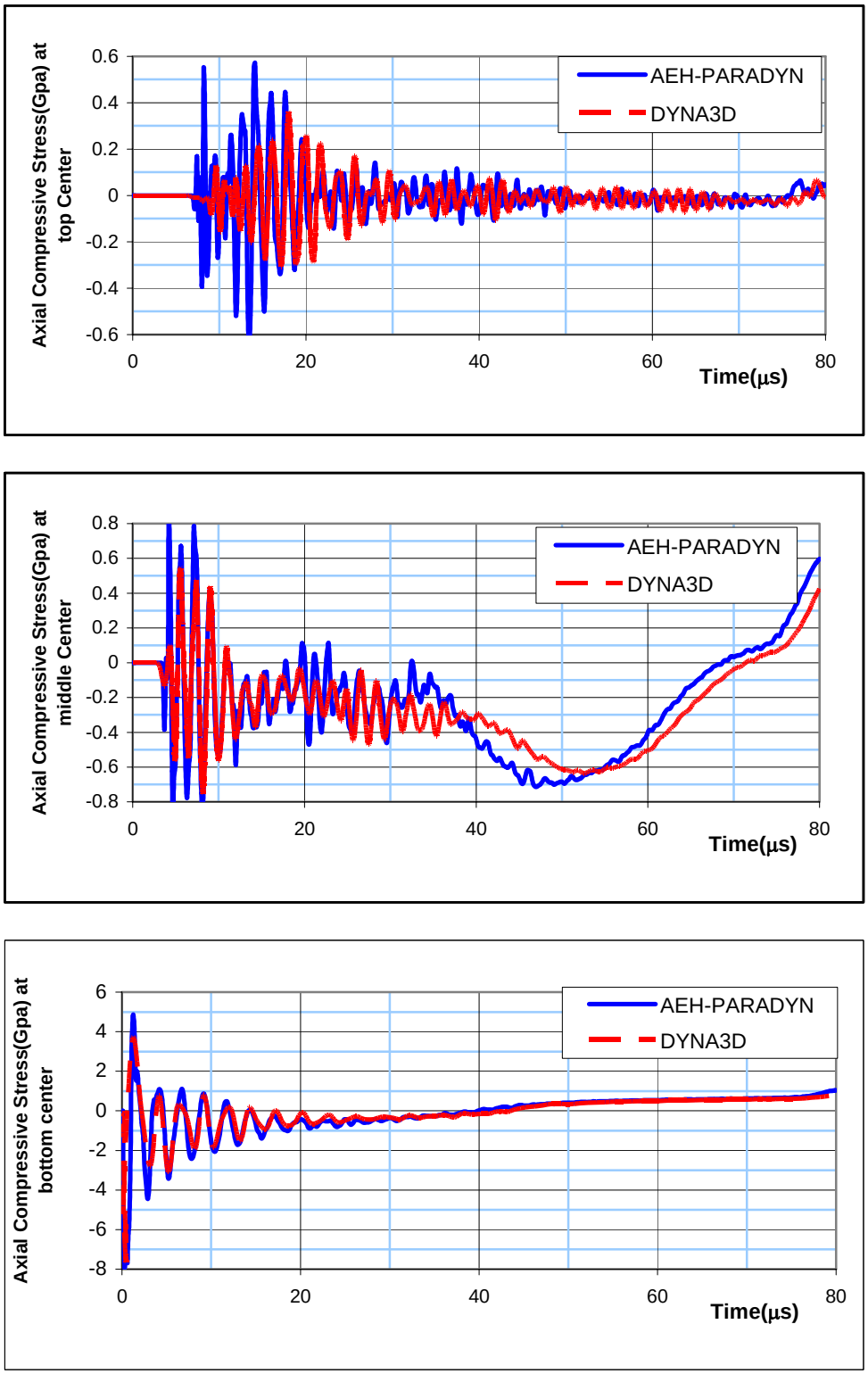

Figure 8. DYNA3D and AEH-PARDYN axial stress solutions for the validation problem.

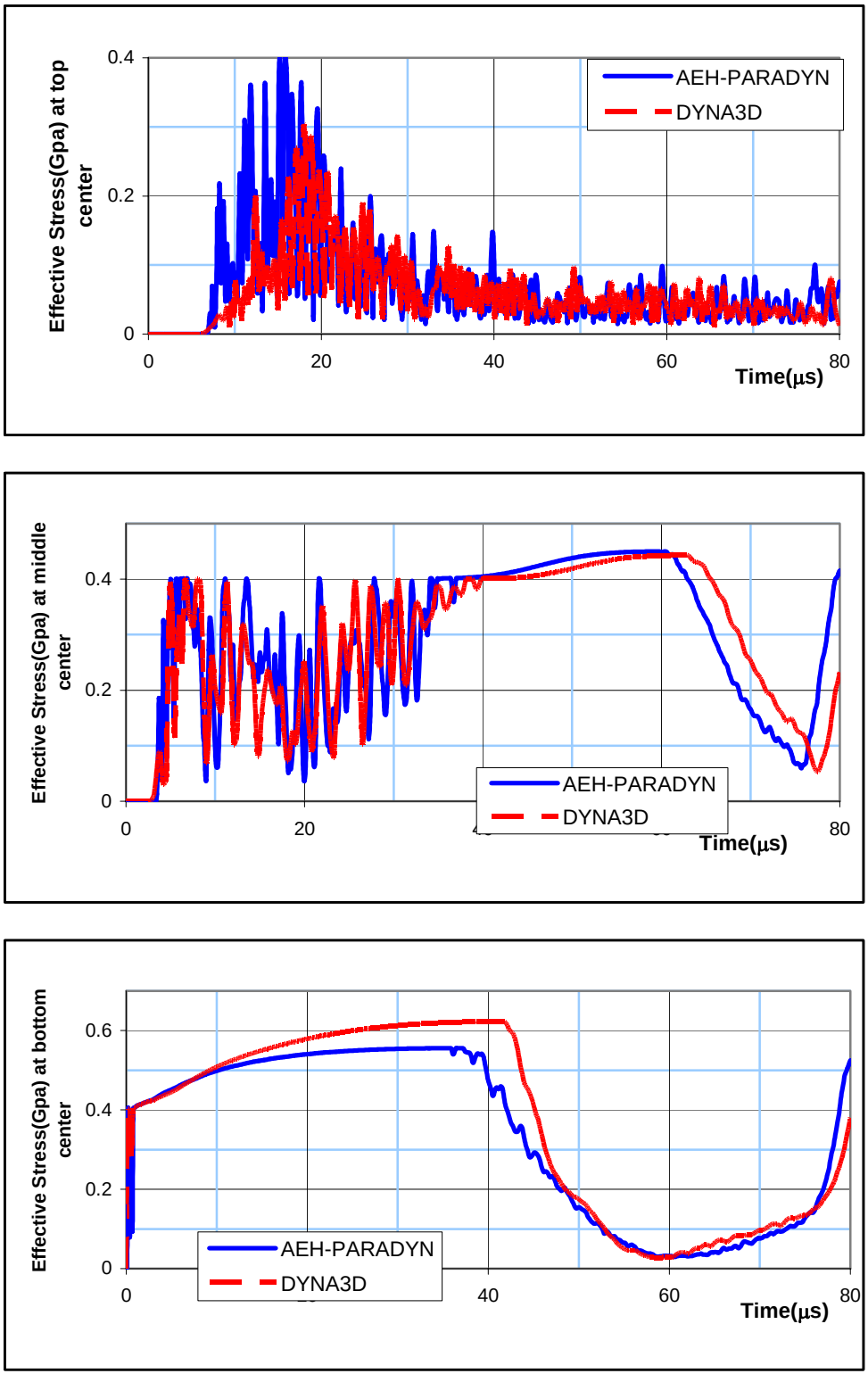

Figure 9. DYNA3D and AEH-PARDYN effective stress solutions for the validation problem.

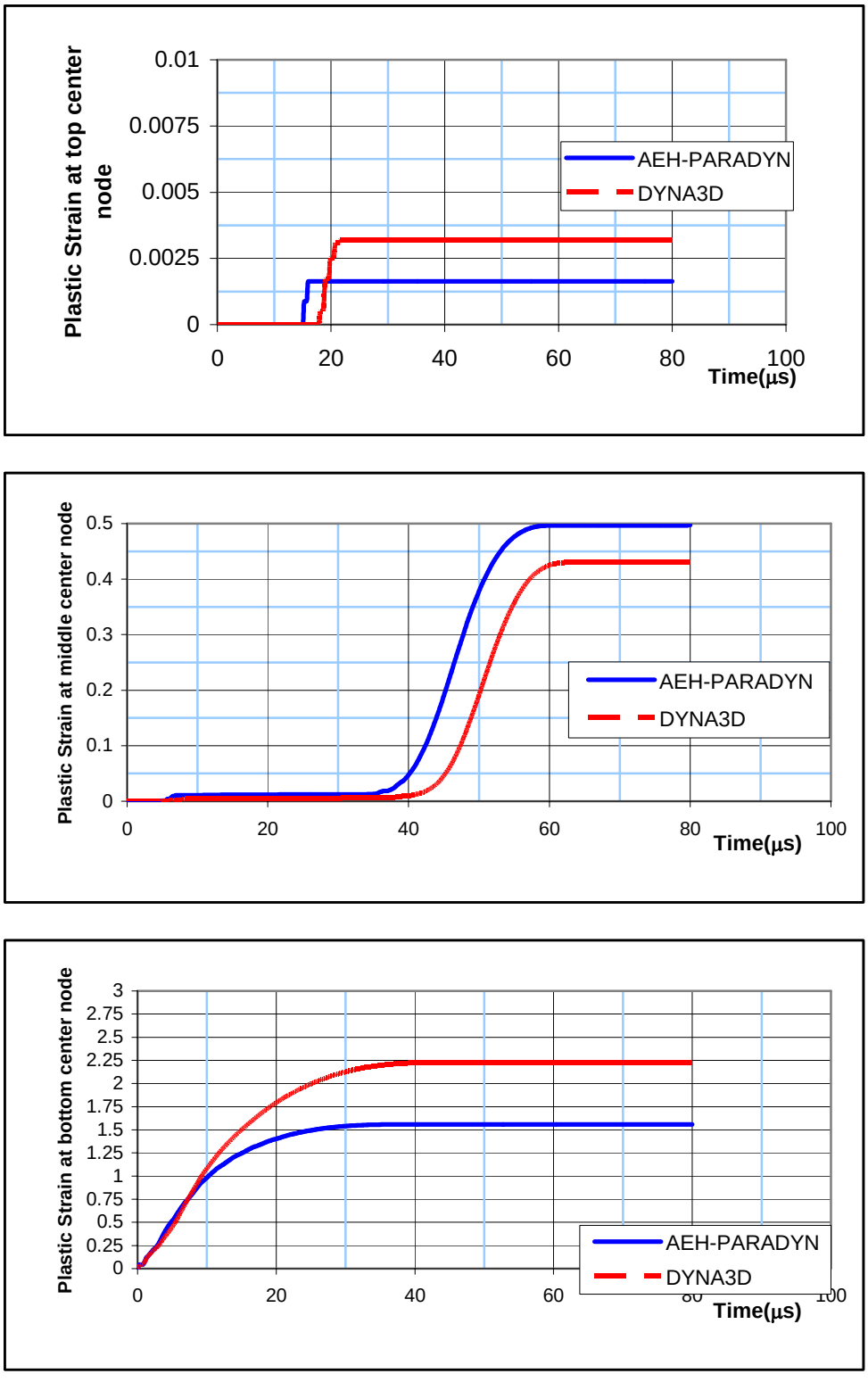

Figure 10. DYNA3D and AEH-PARDYN effective plastic strain solutions for the validation problem

Table 3. Wall clock times for scalability study.

Nodes	Elements	No. of Processors	Wall Clock Time
9787	8064	4	3072
18758	16128	8	4051
35321	31240	16	6046
71217	64512	32	7492
137538	127050	64	8944
140727	122880	8	88369
140727	122880	16	44376
140727	122880	32	22303
140727	122880	64	11353

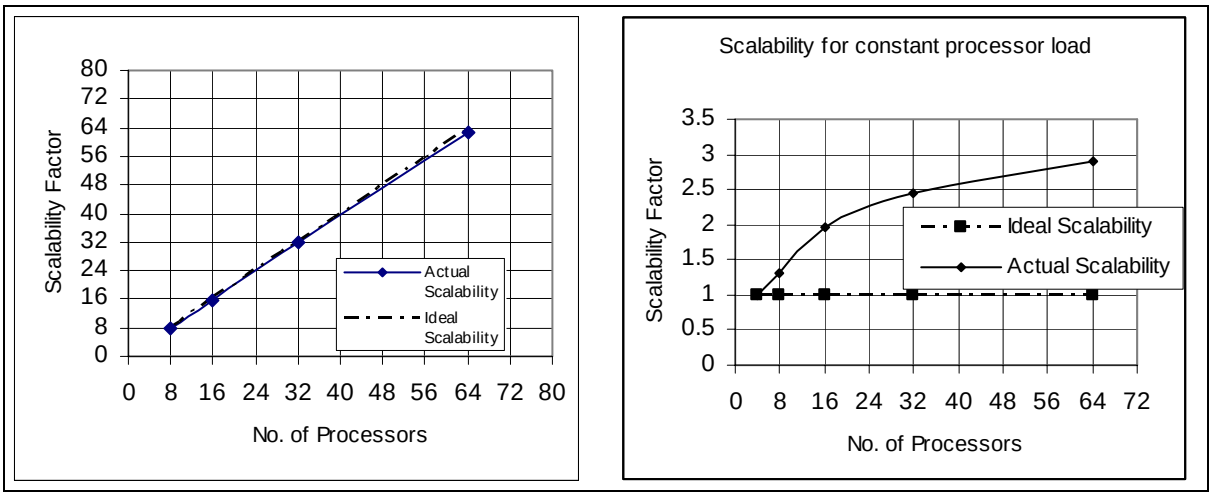

Figure 11. Scalability results for a fixed mesh and for a constant processor load.

In these laminates, a basic unit consisting of a soft layer and a hard layer is repeated a number of times. Laminates are then bonded to soft buffer layers and mounted on to back plates. The soft layer is a polycarbonate (PC) plastic sheet of 0.74-mm thickness. Different materials and thicknesses are used for the hard layers as follows: aluminum (0.37-mm thickness), steel (0.37-mm thickness), and glass (0.55-mm thickness). The soft buffer layer has a thickness of 0.74 mm and is made from PC. The back plate has a thickness of 12.5 mm and is made from polymethyl methacrylate plastic. As shown in figures 12–14, the laminates are impacted in a direction normal to the lay-up using flyer plates made of PC. The flyer plate has a thickness of 2.87 mm. The diameters of the flyer plates, laminates, and the back plates are 34, 38.1, and 38.1-mm, respectively. The details of the three laminate constructions are in table 4.

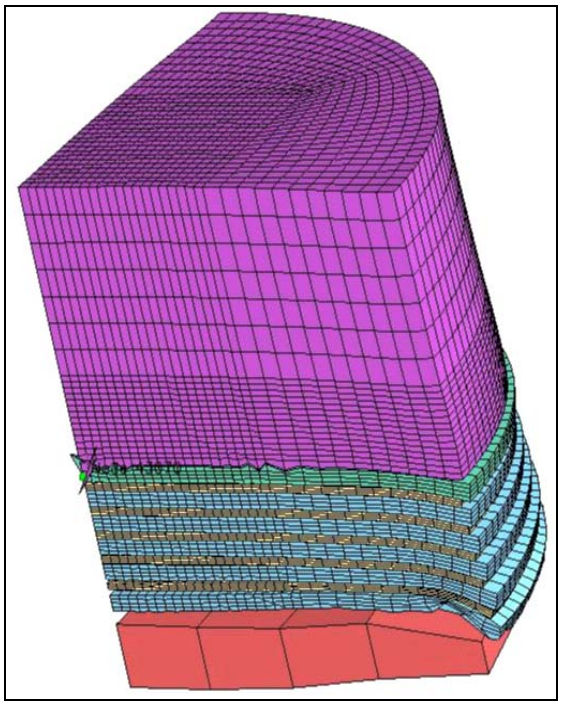

Figure 12. Finite-element mesh for PC74AL37 laminate and its buffer layer, back plate, and flyer.

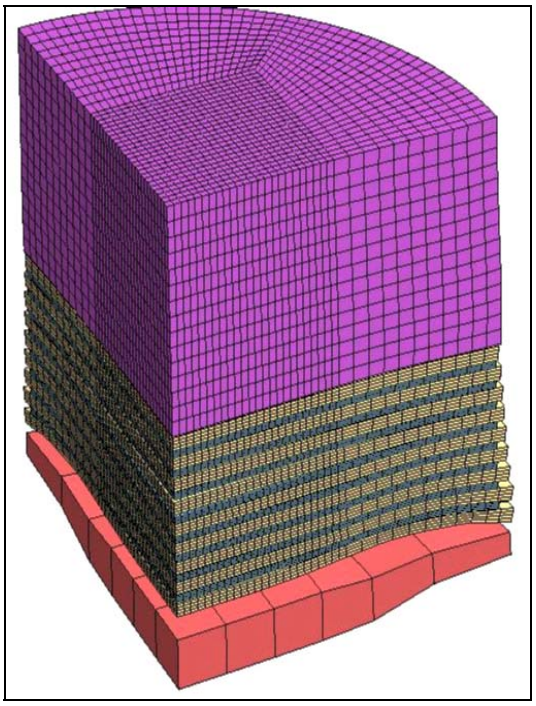

Figure 13. Finite-element mesh for PC74SS37 laminate and its buffer layer, back plate, and flyer.

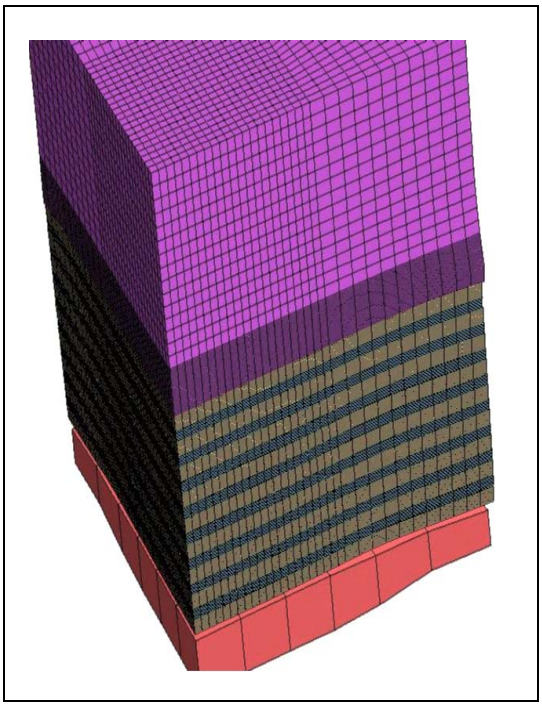

Figure 14. Finite-element mesh for PC74GS55 laminate and its buffer layer, back plate, and flyer.

Table 4. Laminate and impact velocity details.

Laminate Types	No. of Repeating Units	Laminate Thickness Including Buffer Layer (mm)	Flyer Plate Velocity (m/s)
PC74AL37	5	6.62	589
PC74SS37	8	9.97	561
PC74GS55	7	9.95	563

As can be seen from the deformed meshes in figures 12–14, different meshes are used for the three laminates. The PC74AL37 laminate, including its buffer layer, back plate, and the flyer plate, were all meshed with a total of 69899 nodes and 55095 elements. The PC74SS37 laminate and buffer, back, and flyer plates were meshed with a total of 108326 nodes and 82827 elements. Finally, the PC74GS55 laminate's impact was modeled with a total of 167549 nodes and 141798 elements. Because the experiments showed much delamination, and because the interlaminar strengths of the laminates are relatively small, i.e., when compared to the impact generated loads, laminar interfaces were used and modeled as zero strength slide surfaces. The effect of these slide surfaces can be seen as outflowing layers in the deformed meshes in figures 12–14. The material properties used for the present simulations are in table 5.

Table 5. Material properties.

Material	Density (g/m^3)	Shear Modulus (GPa)	Yield Stress (GPa)	Plastic Modulus (GPa)	Poisson's Ratio
PC	1190	0.94	0	1.60	0.37
PMMA	1180	1.20	0	1.60	0.34
6061 AL	2710	30.0	0.32	0.69	0.33
304 SS	7890	77.0	0.33	1.7	0.29
D 263 glass	2510	30.1	—	—	0.208

Before conducting the dual level macro/micro analyses with AEH-PARADYN, single level DYNA3D global analyses were conducted using the aforementioned finite-element models. Using DYNA3D's elastic/plastic material Model 3, for layer materials, the laminate is treated as materially heterogeneous. The results for the axial velocity at the back of the buffer layer are compared with the experimental results in figures 15–17. Even though the overall trends of loading and unloading of the shock wave are predicted well, there is much discrepancy in the predictions of the initial slope and the peak velocity reached.

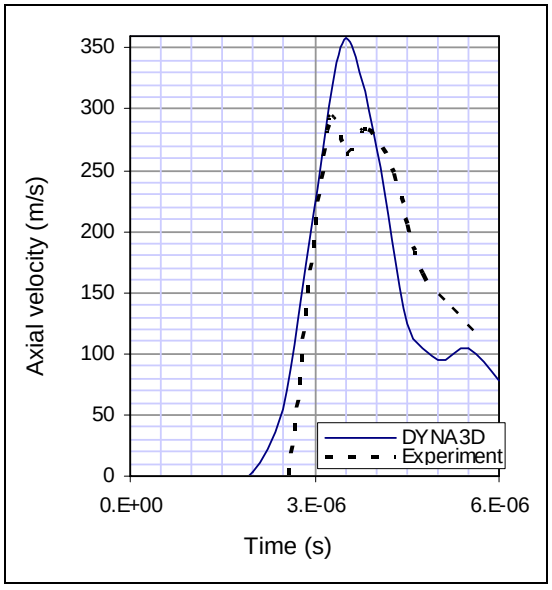

Figure 15. Experimental result and DYNA3D prediction for axial velocity at the back of buffer layer for the PC74AL37 laminate.

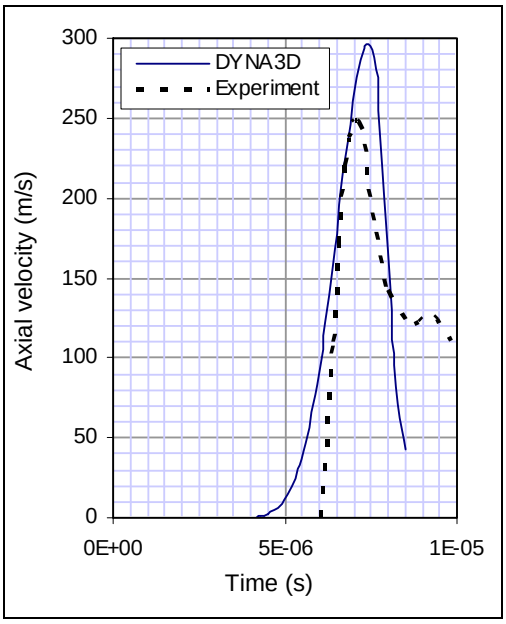

Figure 16. Experimental result and DYNA3D prediction for axial velocity at the back of buffer layer for the PC74SS37 laminate.

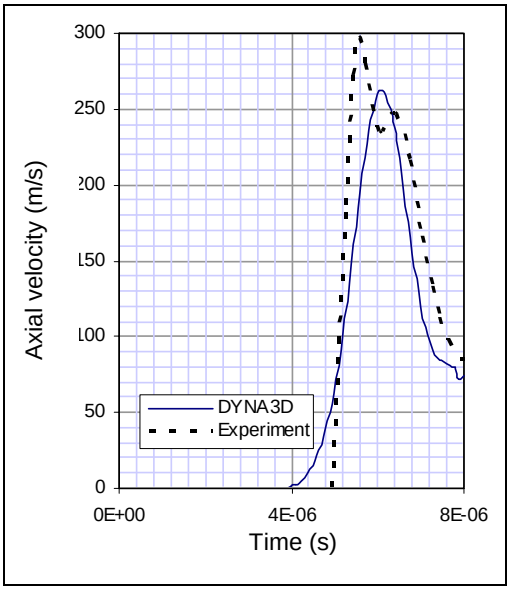

Figure 17. Experimental result and DYNA3D prediction for axial velocity at the back of buffer layer for the PC74GS55 laminate.

The AEH-PARADYN analyses were run assuming that the laminates were all homogeneous in the global sense, but heterogeneous at microlevel. Two-layer microstructural AEH models were used to bring in the lamination effect of the hard and soft layers. At the microlevel, the layer

constituents are assumed to exhibit elastic/plastic behavior that is similar to the DYNA3D's elastic/plastic Material Type 3. The predictions from these analyses for the axial velocity at the back of the buffer layer are compared with the experimental results in figures 18–20. For all the three laminates, the predictions compared well, especially in following the initial slope, peak velocity, and the post peak unloading.

This example clearly demonstrates the ability of the AEH microstructural model to accurately predict the shock wave propagation in highly dissimilar layered materials, and the capability of the included AEH microstructural model for conducting multiscale macro/micro analyses with AEH-PARADYN.

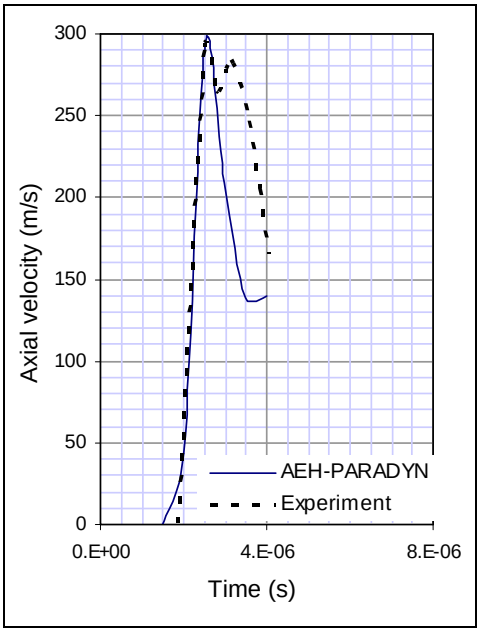

Figure 18. Experimental result and AEH-PARDYN prediction for axial velocity at the back of buffer layer for the PC74AL37 laminate.

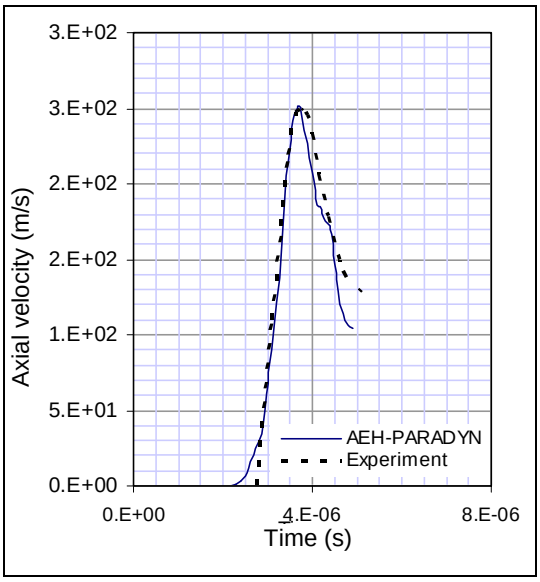

Figure 19. Experimental result and AEH-PARDYN prediction for axial velocity at the back of buffer layer for the PC74SS37 laminate.

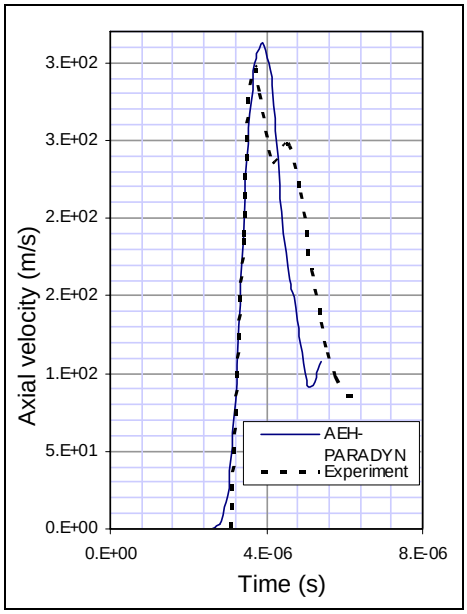

Figure 20. Experimental result and AEH-PARDYN prediction for axial velocity at the back of buffer layer for the PC74GS55 laminate.

5. Future Work and Conclusions

Microstructures are features of the U.S. Army's advanced structures and armor materials. Homogenization theories such as the AEH are being developed to model the effects of these microstructures on global material and structural responses. With the present coupling of the AEH-based microstructural model in PARADYN, many in-situ material responses can be studied under diverse global structural conditions. The sample applications presented in this report demonstrate this. Efforts underway include the following extensions to this work:

- using PARADYN's diverse material library to model different microphase materials,
- modifying the AEH model used in this work to include an equation of state, and
- extending the application range to include complex microstructures and diverse global applications.

6. References

Bensoussan, A.; Lions, J. L.; Papanicolaou, G. Asymptotic Analysis for Periodic Structures; New York: North Holland Publishing Co., 1978.

Chung, P. W.; Namburu, R. R.; Tamma, K. K. Three-Dimensional Elasto-Plastic Heterogeneous Media Subjected to Short Transient Loads. *AIAA Paper-99-1239* **1999**.

Clarke, J. A.; Namburu, R. R. A Distributed Computing Environment for Interdisciplinary Applications. *Concurrency and Computation: Practice and Experience*; *Cocurrency Computa: Pract. Exper*. **2002**, 14, 1161–1174.

Fish, J.; Shek, K.; Pandheeradi, M.; Shepard, M. Computational Plasticity for Composite Structures based on Mathematical Homogenization: Theory and Practice. *Computer Methods in Applied Mechanics and Engineering* **1997**, *148*, (1–2), 53–73.

Ghosh S.; Moorthy, S. Elasto-Plastic Analysis of Arbitrary Heterogeneous Materials With the Voronoi Cell Finite-Element Method. *Computer Method in Applied Mechanics and Engineering* **1995**, *121*, 373–409.

Guedes, J. M.; Nikuchi, N. Preprocessing and Post-Processing for Materials Based on the Homogenization Method With Adaptive Finite-Element Methods. *Computer Methods in Applied Mechanics and Engineering* **1990**, *83*, (2), 143–198.

Hashin, Z. The Elastic Modulii of Heterogeneous Materials. *ASME J. Appl. Mech.* **1962**, *29*, 143–150.

Hashin, Z.; Strickman, S. A. Variational Approach to the Theory of the Elastic Behavior of Multiphase Materials. *Journal Mech. Phys. Sol.* **1963**, *11*, 127–140.

Hill, R. Theory of Mechanical Properties of Fiber Toughened Materials. *J. Mech. Phys. Sol.* **1964**, *12*, 99–212.

Lene, F. Contribution à Lètude des Matériaux Composites et de Leur Endommagement. Thesis, Université Paris 6, 1984.

Lene, F. Damage Constitutive Relations for Composite Materials. *Engineering Fracture Mechanics* **1986**, *25*, (5/6), 713–728.

Licht Frottement, C. Viscoplasticité et Homogenization. Thesis, Université Montpellier 2, 1987.

Moulinec, M.; Suquet, P. A Fast Numerical Method for Computing the Linear and Nonlinear Mechanical Properties of Composites. *C. R. Acad. Sci.* Paris 318, **1994**, 1417–1423.

Namburu, R. R. Unified Finite-element Methodology for Thermal-Structural Problems. Thesis, The University of Minnesota, July 1991.

Sanchez-Palencia, E. Non-Homogeneous Media and Vibration Theory – Lecture Notes in Physics; Springer Verlag, 1980.

Suquet, F. Plasticité et Homogenization. Thesis, Université Paris 6, 1982.

Terada, K.; Kikuchi, N. Nonlinear Homogenization Method for Practical Applications, Computational Methods in Micro-mechanics. *American Society of Mechanical Engineers*, Applied Mechanics Division, **1995**, *212*, 1–16.

Valisetty, R. R.; Namburu, R. R.; Chung, P. W. *Scalable Implementation of Three-Dimensional Heterogeneous Media Subjected to Short Transient Loads*; ARL-TR-2351; U.S. Army Research Laboratory: Aberdeen Proving Ground, MD, 2000.

Willis, J. Elastic Theory of Composites. In *Mechanics of Solids*; Oxford: Pergamon Press, pp 353–386, 1982.

Zhuang, S. Shock Wave Propagation in Periodically Layered Composites. Ph.D. Thesis, California Institute of Technology, Pasadena, CA, 2002.

Appendix. Microstructural Equations

A.1 Governing Equations

These equations are presented in several references, most recently in Chung et al.[1] Assume a three-dimensional body Ω is an assembly of periodic structures containing different materials, as shown in figure A-1. Typically, the unit cell is very small and of order ε (where ε is a small positive number) compared to the dimensions of the problem domain. Structural response quantities such as displacements, velocities, stresses, and strains are assumed to have slow variations (macroscopic) from point to point as well as fast (microscopic) variations within a small neighborhood ε of a given point x. Let Y be a (periodic) representative part of Ω.

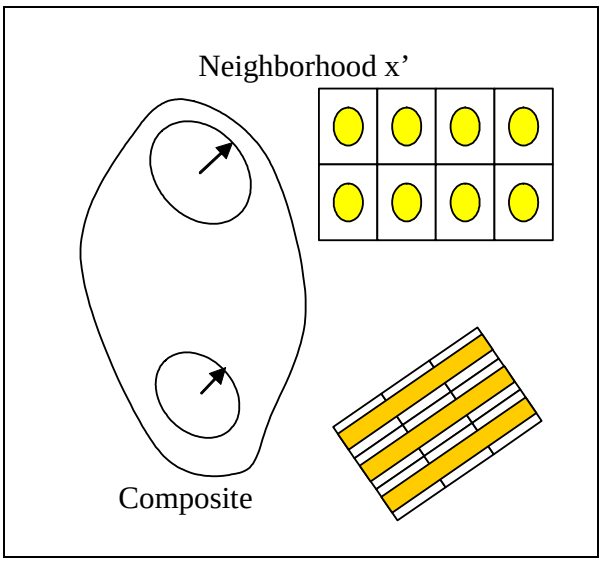

Figure A-1. Macro/microanalyses neighborhoods.

Here we distinguish two scales: the macroscopic scale ($x \in \Omega$) and microscopic scale ($y \in \Omega$). Lagrangian representations of conservation of mass and momentum equations are used. The conservation of mass is used to calculate the current density from the initial density. The momentum equation, the kinematic relations, and the constitutive model are represented by

$$\rho^{\varepsilon}\dot{v}_i^{\varepsilon} - \sigma_{ji,j}^{\varepsilon} = f_i\,, \tag{A-1}$$

$$\dot{e}_{ij}^{\varepsilon} = \frac{1}{2}(v_{i,j}^{\varepsilon} + v_{j,i}^{\varepsilon})\,, \tag{A-2}$$

and

[1]Chung, P. W.; Namburu, R. R.; Tamma, K. K. Three-Dimensional Elasto-Plastic Heterogeneous Media Subjected to Short Transient Loads. *AIAA paper-99-1239* **1999**.

$$\sigma_{ij}^{\varepsilon} = S_{ij}(\dot{e}_{ij}^{\varepsilon}, E), \tag{A-3}$$

where ρ is the density, f_i is the body force vector, E is the internal energy, the superscript ε denote micro/macro continuum solutions, v_i is the velocity vector, σ_{ij} is the stress tensor, and e_{ij} is the strain tensor. The initial conditions in the domain Ω^{ε} and boundary conditions on the surface of the domain $\Gamma\,(=\partial\Gamma_1 \cup \partial\Gamma_2)$ are given by

$$u_i^{\varepsilon}(t=0) = u_{o_i}^{\varepsilon}, \tag{A-4}$$

$$v_i^{\varepsilon}(t=0) = v_{o_i}^{\varepsilon}, \tag{A-5}$$

$$u_i^{\varepsilon} = u_i^{o\varepsilon} \text{ on } \partial\Gamma_1, \tag{A-6}$$

and

$$\sigma_{ji}^{\varepsilon} n_i = T_i \text{ on } \partial\Gamma_2, \tag{A-7}$$

where u_i is the displacement vector and n_i is a surface normal.

A.2 Time Integration

A second-order accurate Lax-Wendroff-based explicit time integration procedure Tamma and Namburu[2] is employed for the conservation equation or equation of motion. In this approach, the dependent variable velocity is first discretized in time using a second order Taylor series expansion.

$$v_i^{\varepsilon^{n+1}} = v_i^{\varepsilon^n} + \Delta t \dot{v}_i^{\varepsilon^{n+1/2}}. \tag{A-8}$$

Taking appropriate time derivatives of equation 1 and substituting for the velocity and acceleration gives

$$\rho v_i^{\varepsilon^{n+1}} - \rho v_i^{\varepsilon^n} = \left(\sigma_{ji,j}^{\varepsilon^{n+1/2}} + \rho f_i^{n+1/2}\right)\Delta t\,. \tag{A-9}$$

The stress increment is related to a strain increment through an appropriate constitutive equation. The elasto-plastic constitutive equation at midpoint time increment is defined by

$$\sigma_{ij}^{\varepsilon^{n+1/2}} = M_{ijkl}(\sigma_{ij}^{\varepsilon^{n-1/2}} + C_{klmn}\dot{\varepsilon}_{mn}^{\varepsilon^{n-1/2}}\Delta t^{n+1/2}), \tag{A-10}$$

where M_{ijkl} and C_{ijkl} are radial return in plasticity tensor and elasticity tensor.

Stresses and strain rates at midpoint time can be evaluated using the predicted displacements as shown by

[2]Tamma, K. K.; Namburu, R. R. A Robust Self Starting Explicit Computational Methodology for Structural Dynamic Applications: Architecture and Representations. *International Journal for Numerical Methods in Engineering* **1990**, *29*, 1441–1454.

$$u_i^{\varepsilon^{n+1/2}} = u_i^{\varepsilon^n} + \frac{\Delta t}{2} v_i^{\varepsilon^{n+1/2}} . \tag{A-11}$$

A.3 Asymptotic Expansion and Elasto/plastic Constitutive Equations

The homogenization method is based on the asymptotic expansion of the primary variables together with a unit cell approach for a heterogeneous structure. Assume a 3-D body Ω is an assembly of periodic structures. Typically, the unit cell is very small, of order ε (ε is a small positive number) compared to the dimensions of the problem domain. Typically, two-scale asymptotic expansion can be employed to approximate the displacement, velocity, strain, or stress fields.

$$u_i^{\varepsilon}(x,y) = u_{o_i}(x,y) + \varepsilon u_{1_i}(x,y) + \varepsilon^2 u_{2_i}(x,y) + \cdots, \tag{A-12}$$

$$v_i^{\varepsilon}(x,y) = v_{o_i}(x,y) + \varepsilon v_{1_i}(x,y) + \varepsilon^2 v_{2_i}(x,y) + \cdots, \tag{A-13}$$

$$e_i^{\varepsilon}(x,y) = e_{o_i}(x,y) + \varepsilon e_{1_i}(x,y) + \varepsilon^2 e_{2_i}(x,y) + \cdots, \tag{A-14}$$

and

$$\sigma_i^{\varepsilon}(x,y) = \sigma_{o_i}(x,y) + \varepsilon \sigma_{1_i}(x,y) + \varepsilon^2 \sigma_{2_i}(x,y) + \cdots, \tag{A-15}$$

where $u_i^{\varepsilon}(x,y)$, $v_i^{\varepsilon}(x,y)$, $e_i^{\varepsilon}(x,y)$, and $\sigma_i^{\varepsilon}(x,y)$ are Y-periodic functions.

The asymptotic expansion homogenization (AEH) approach for nonlinear applications is based on the instantaneously linearized assumption for the constitutive model.[3] The fundamental assumption of the AEH approach, therefore, is that the true solution in the ε space is decomposed into a macro space *x* and a micro space *y*. The basic assumption here is that multiple scales exist only in the spatial variables and that no such scaling exists for the time variable. Further reading in space and time asymptotic expansion approaches can be found in Bensoussan.[4] The general approach to heterogeneous problems is to separate and draw clear distinction between the micro- and macrolevel equilibrium equations regardless, per the earlier linearized assumption, of material nonlinearity. This is accomplished by asymptotically expanding the primary variables where the asymptotic scale is approximated to the second order.

$$v_i^{\varepsilon}(x,y) = v_{o_i}(x,y) + \varepsilon v_{1_i}(x,y) + \varepsilon^2 v_{2_i}(x,y) + \cdots . \tag{A-16}$$

Spatial gradients in ε-space are taken with respect to the *x*-coordinate system. The corresponding gradient for Y-periodic functions (where micro and macro are now distinguishable) is given by the chain rule where the scaling is defined by $y = x/\varepsilon$; hence, for any Y-periodic function ϕ, the earlier gradients are replaced by

[3]Terada, K.; Kikuchi, N. Nonlinear Homogenization Method for Practical Applications, Computational Methods in Micro-mechanics. *American Society of Mechanical Engineers*, Applied Mechanics Division, **1995**, 212, 1–16.

[4]Bensoussan, A.; Lions, J. L.; Papanicolaou, G. *Asymptotic Analysis for Periodic Structures*; New York: North Holland Publishing Co., 1978.

$$\frac{d\phi}{dx_i} = \frac{\partial \phi}{\partial x_i} + \frac{1}{\varepsilon}\frac{\partial \phi}{\partial y_i}. \tag{A-17}$$

Then, using equation A-1 in equation A-7 while considering equation A-2 gives the rate of strain tensor defined by

$$\dot{\varepsilon}_{ij}^{\varepsilon} = [e_{ij}^{x}(v_o) + e_{ij}^{y}(v_1)] + \varepsilon[e_{ij}^{x}(v_1) + e_{ij}^{y}(v_2)] + \cdots, \tag{A-18}$$

where the symmetrized gradient tensors, e^{x}_{ij} and e^{y}_{ij} are defined by

$$e_{ij}^{x}(\phi) = \frac{1}{2}\left(\frac{\partial \phi_i}{\partial x_j} + \frac{\partial \phi_j}{\partial x_i}\right) \tag{A-19}$$

and

$$e_{ij}^{y}(\phi) = \frac{1}{2}\left(\frac{\partial \phi_i}{\partial y_j} + \frac{\partial \phi_j}{\partial y_i}\right). \tag{A-20}$$

The relevant expressions for gradients and velocities are first substituted into the governing equations of motion. Next, the micro and macro equations are identified by selecting the appropriate coefficients to the scaling factors ε which must each be identically zero. Substituting the asymptotically-expanded velocities, equation A-1, in the strain rate, equation A-3, and then using the constitutive equation, equation A-16, in the equations of motion, equation A-15, yields a set of equations dependent on powers of ε. To satisfy the equations of motion, each term associated with each of the powers of ε must approach zero identically. This leads to a set of equations associated with the microscopic and macroscopic equations of motion. The first equation, associated with the powers of ε^{-2}, is given by

$$\varepsilon^{-2}: \quad \frac{\partial}{\partial y_j} C_{ijkl}^{*} \frac{\partial v_{o_k}^{n-1}}{\partial y_l} = 0, \tag{A-21}$$

where $C_{ijkl}^{*} = M_{ijpq} C_{pqkl}$. Equation A-21 states that $v_{o_i}^{n-1}$ is a function only of *x*. Hence, derivatives of *y* are zero. Using this inference, the equation associated with the powers of ε^{-1} is derived as

$$\varepsilon^{-1}: \quad \frac{\partial}{\partial y_j} C_{ijkl}^{*} \frac{\partial v_{o_k}^{n-1}}{\partial x_l} + \frac{\partial}{\partial y_j} C_{ijkl}^{*} \frac{\partial v_{1_k}^{n-1}}{\partial y_l} = -\frac{1}{\Delta t}\frac{\partial}{\partial y_j}(M_{ijkl}\sigma_{kl}^{n-1/2}). \tag{A-22}$$

Equation A-22 relates the perturbative velocity field, v_1, to the macroscopic velocity field, v_0. The equation relating these two quantities will become the important micro/macroequation, providing the direct link to relate microscopic to the macroscopic velocities. It provides the corrections which account for the shape of the interface separating various phases and the time-dependent plastic softening effect due to material nonlinearities. For a homogeneous material problem, where gradients over *y* of $C_{ijkl}^{*}\partial v_{o_i}^{n-1} / \partial x_l$ are zero, and in which plastic effects have no *y*

dependence, the solution to equation A-22 $v_{1_i}^{n-1}$ is identically zero. In the special case where no plastic yielding occurs, the problem degenerates to a transient elastic homogenization problem.

Finally, the equation associated with the powers of ε^o is written as

$$\begin{aligned}\varepsilon^0: \quad & \frac{\partial}{\partial x_j} C^*_{ijkl} \frac{\partial v^{n-1}_{o_k}}{\partial x_l} + \frac{\partial}{\partial x_j} C^*_{ijkl} \frac{\partial v^{n-1}_{1_k}}{\partial y_l} \\ & + \frac{\partial}{\partial y_j} C^*_{ijkl} \frac{\partial v^{n-1}_{o_k}}{\partial x_l} + \frac{\partial}{\partial y_j} C^*_{ijkl} \frac{\partial v^{n-1}_{2_k}}{\partial y_l} \\ & = \frac{\rho}{\Delta t^2} \Delta v^{n+1}_{o_i} - \frac{1}{\Delta t} \frac{\partial}{\partial x_j} M_{ijkl} \sigma^{\varepsilon^{n-1/2}}_{kl} - \frac{\rho}{\Delta t} f_i^{n+1/2}.\end{aligned} \tag{A-23}$$

Much like equation A-22 provided the basis for the microscale problem, equation A-23 provides the basis for the macroscale problem. By taking the volume average of equation A-23, substituting for v_1 using the solution of equation A-22 and noting the periodicity, the final governing equation of motion is given by

$$\langle \rho \rangle \Delta v^{n+1}_{o_i} = \Delta t \frac{\partial}{\partial x_j} \left\langle \sigma_{ij}^{n+1/2} + \sigma_{ij}^c \right\rangle + \Delta t \langle \rho \rangle f_i^{n+1/2}, \tag{A-24}$$

where the "corrector stress," σ_{ij}^c, is defined by

$$\sigma_{ij}^c = C^*_{ijkl} \frac{\partial v^{n-1}_{1_k}}{\partial y_l}, \tag{A-25}$$

and where quantities in brackets denote

$$\langle (\ ) \rangle = \frac{1}{V} \int_Y (\ ) dY. \tag{A-26}$$

It is of interest to note that equation A-24, for heterogeneous conditions, is similar in form to equation A-6, the homogeneous equation, making the integration of a micromechanical problem into a macroanalysis tractable and straightforward.

A.4 Constitutive Equation: Elasto/Plastic

The stress tensor is split into two parts. The first part, S_{ij}, is deviatoric stress, which is related to material strength, and the second part is pressure, P. To simplify notation, the superscript ε has been omitted.

$$\sigma_{ij} = -\delta_{ij} P + S_{ij} \tag{A-27}$$

and

$$\frac{1}{3} \sigma_{ii} = -P. \tag{A-28}$$

The first term in equation A-27 accounts for volumetric changes and is typically evaluated from equations of state in explicit dynamics. The second term, the stress deviator, is related to the deformation of the material and is defined by a constitutive model, and in particular, the time rate of change of the deviator is evaluated from the strain rates.

$$S_{ij} = 2G\varepsilon_{ij} + \Delta_{ij} . \tag{A-29}$$

This model can be defined with any number of local nodes, elements, and materials, but since this model is called repeatedly for each time step, for each element for which microstructural response is deemed important, a complex microstructure model can overwhelm the overall computations, therefore keeping the model simple is important. Δ_{ij} is the correction for rigid body rotation.

An isotropic hardening model with a rate-dependent Von-Mises yield condition is employed in the present analysis. A consistency condition ensures that the stress state remains on the yield surface at the start and end of a time-step. Such a condition is given by

$$R^{n+1}Q_{ij} = S_{ij}^{n+1} . \tag{A-30}$$

The variable R is the rate-dependent radius of the yield surface or the apparent yield stress, Q_{ij} is the vector specifying the normal direction to the yield surface, and S_{ij} is the deviatoric component of the stress. The stresses are understood to be the co-rotated second-order tensor according to the Jaumann definition of the co-rotational derivative. The Jaumann derivative of the Cauchy stress, $\dot{\sigma}^{j}_{ij}$, is related to the material time derivative, $\dot{\sigma}_{ij}$, by

$$\dot{\sigma}^{J}_{ij} = \dot{\sigma}_{ij} + \sigma_{ik}\omega_{kj} + \omega_{ik}\sigma_{kj} , \tag{A-31}$$

where ω_{ij} is the rotation tensor, the standard skew-symmetric component of the velocity gradient. The radius of the yield surface is defined by

$$R = \sigma_Y^o \left[1 + \left(\frac{\bar{e}}{D} \right)^{\frac{1}{p}} \right] + H'\bar{\varepsilon}^{p} , \tag{A-32}$$

where σ^{y}_{o} is the static yield stress of the material, and D and p are the so-called fluidity parameters. H' is the hardening parameter, and $\bar{\varepsilon}^{p}$ is the effective plastic strain. The effective rate of deformation, $\bar{\varepsilon}$, is defined by

$$\bar{e} = \sqrt{\frac{2}{3}\dot{e}_{ij}\dot{e}_{ij}} , \tag{A-33}$$

where e_{ij} is the deviatoric component of the total strain, ε_{ij}. The normality condition, specified by the normal vector Q_{ij}, is given by

$$Q_{ij} = \frac{S_{ij}}{\sqrt{S_{mn}S_{mn}}} . \tag{A-34}$$

For a homogeneous material (which is applicable in the present derivation since the constitutive equations are applied at the microlevel where the material is homogeneous within each phase), the incremental relationships for the apparent yield stress and the deviatoric stress are defined as

$$R^{n+1} = R^n + \frac{2}{3} H' \Delta\lambda \tag{A-35}$$

and

$$S_{ij}^{n+1} = S_{ij}^{n+1^T} - 2G\Delta\lambda Q_{ij}\,, \tag{A-36}$$

where $S_{ij}^{n+1^T}$ is the deviatoric trial stress, $\Delta\lambda$ is a scalar quantity representing the magnitude of the radial return correction due to plastic yielding, and G is the elastic shear modulus. The deviatoric trial stress is defined by

$$S_{ij}^{n+1^T} = S_{ij}^{n} + C_{ijkl}\dot{e}_{kl}^{n}\Delta t\,, \tag{A-37}$$

where C_{ijkl} is the tensor containing elastic properties.

Finally, substituting equation A-37 and A-35 into equation A-30 and solving for the radial return correction parameter gives

$$\Delta\lambda = \frac{3/2}{(3G + H')}\left(\sqrt{\frac{3}{2} S_{ij}^{n+1^T} S_{ij}^{n+1^T}} - R_n\right). \tag{A-38}$$

Using equation A-38 in equation A-36 and employing the standard assumption that a material is elastic in its dilatational behavior and plastic only in shear gives the total stress increment in equation A-16. The constitutive equation A-16 can now be employed in the derivation of the micro and macro governing equations.

NO. OF COPIES ORGANIZATION

1 (PDF ONLY) DEFENSE TECHNICAL INFORMATION CTR
DTIC OCA
8725 JOHN J KINGMAN RD
STE 0944
FORT BELVOIR VA 22060-6218

1 US ARMY RSRCH DEV & ENGRG CMD
SYSTEMS OF SYSTEMS INTEGRATION
AMSRD SS T
6000 6TH ST STE 100
FORT BELVOIR VA 22060-5608

1 INST FOR ADVNCD TCHNLGY
THE UNIV OF TEXAS
AT AUSTIN
3925 W BRAKER LN STE 400
AUSTIN TX 78759-5316

1 US MILITARY ACADEMY
MATH SCI CTR EXCELLENCE
MADN MATH
THAYER HALL
WEST POINT NY 10996-1786

1 DIRECTOR
US ARMY RESEARCH LAB
IMNE ALC IMS
2800 POWDER MILL RD
ADELPHI MD 20783-1197

3 DIRECTOR
US ARMY RESEARCH LAB
AMSRD ARL CI OK TL
2800 POWDER MILL RD
ADELPHI MD 20783-1197

3 DIRECTOR
US ARMY RESEARCH LAB
AMSRD ARL CS IS T
2800 POWDER MILL RD
ADELPHI MD 20783-1197

NO. OF COPIES ORGANIZATION

ABERDEEN PROVING GROUND

1 DIR USARL
AMSRD ARL CI OK TP (BLDG 4600)

INTENTIONALLY LEFT BLANK.